Preliminary Design of Offshore Wind Turbine Support Structures: The Importance of Proper Mode Shape Estimation

P. van der Male
Offshore Wind Group
Department of Offshore Engineering
Technical University of Delft
p.vandermale@tudelft.nl

Abstract

Offshore wind turbines are highly exposed to time-varying loads. For support structures, estimation of the fatigue damage during the lifetime of the structure is an essential design aspect. This already applies for the preliminary design stage. In determining the dynamic amplification in the frequency domain, modal analysis is a common tool. This paper describes a main drawback of the application of modal analysis in preliminary support structure design. Exact mode shapes are not available, due to the concentrated inertia of the *rotor nacelle assembly* (RNA). Generally the mode shapes of a cantilever beam are applied, in which the RNA mass is neglected. In analyzing three turbine types (V90-3.0MW, SWT-3.6-107 and NREL 5-MW), an overestimation of dynamic amplification due to sea level loading is observed. Estimation of the structural response at the second natural frequency turns out to be poor. Within the range of considered RNA masses, the actual magnitude of the tower top mass does affect the relative error of the modal analysis much. Besides, by increasing the tower and support structure stiffness, the relative error diminishes.

Keywords: offshore wind, support structure, preliminary design, fatigue, frequency domain.

1 Introduction

In preliminary support structure design for offshore wind turbines, frequency domain analysis potentially is a powerful tool to estimate lifetime fatigue damage [7, 11]. Compared to time domain analysis, computational effort can be saved and hence increased opportunities for design optimization exist.

The commonly applied approach for frequency domain analysis in the preliminary support structure design phase is modal analysis [1]. However, the structural characteristics of a traditional offshore wind support structure do not suit the modal analysis procedure very well, due to the presence of the concentrated mass and dashpot at the free end [8]. Moreover, since the system is damped non-classically, the assumption that the structural motion is dictated by classical normal modes is not valid [3].

This paper presents the results of a comparative study between structural response determined with modal analysis and the exact response determined on the basis of direct Fourier transformation. The objective is to establish to what extent the application of estimated modes in modal analysis leads to inaccurate response estimation. The independent variables on which this study is based are the RNA, the first natural frequency of the system and the load positioning, either at the tower top, or at mean sea level. For this purpose, a simple continuous 1D wind turbine model is adopted, consisting of a prismatic cantilever beam with a concentrated mass at the free end. This model typically represents a wind turbine with monopile support structure. Structural motion is restricted to the fore-aft modes and only steady state response is considered. RNA characteristics are varied by considering three turbine types: V90-3.0MW, SWT-3.6-107 and NREL 5-MW. The model is evaluated analytically.

This defined model is applicable for the preliminary design phase. Its simplicity enables straightforward comparison of the calculation methods. Whether the calculated structural response coincides with the actual response, to be obtained via measurements, highly depends on the accuracy of the defined structural characteristics.

2 Model description

The support structure is modelled by means of a prismatic cantilever beam of length L, as depicted

in Figure 1. Within this one-dimensional model, the x-axis coincides with the neutral axis of the undeformed beam. The lateral deflection w is a function of the free variables x and time t. EI represents the bending stiffness of the beam, ρ is the material density and A the cross sectional area. Linear elasticity is assumed, which implies that EI is constant, irrespective of the occurring deformation. Structural damping, incorporated by c_d, represents damping effects due to internal material friction and dissipation of energy at joints. Damping due to soil-structure and fluid-structure interaction is generally superposed to the structural damping [7].

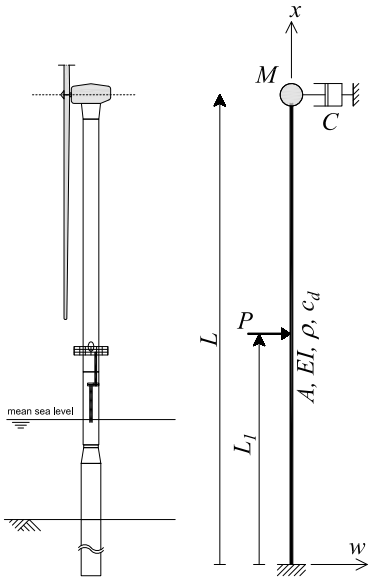

Figure 1: Representation of support structure model.

In order to take into account the dynamic effects of the RNA, the concentrated mass M and viscous damping C are added to the free end of the cantilever beam. The numerical values of these parameters are determined on basis of an assumed rigid rotor. Effects of rotor flexibility are already processed in the tower top loading. The model can be extended by considering the rotary inertia of the RNA and the compressive force in the tower. This comparative study in this paper however, is limited to the disturbing effect of the RNA mass, which is thought to affect the structural response most.

To investigate the response to either wind, wave or ice loads, the external force P is imposed on the model. The position of this force is determined by the length L_1, measured from the origin of the x-w coordinate system.

2.1 Equation of motion

As the angle between the deformed neutral axis and the x-axis is assumed to be close to zero, the system of Figure 1 can be described on the basis of geometrical linearity, which results in a single equation of motion for a continuous system. Similar systems have been described many times, for instance in [9], where use is made of the Kronecker Delta function to generate homogeneous boundary conditions.

On this bases, the equation of motion as adopted for this research becomes

$$\begin{aligned} EI\frac{\partial^4 w}{\partial x^4} =& -\rho A\frac{\partial^2 w}{\partial t^2} - c_d\frac{\partial w}{\partial t} \\ & - \delta(x-L^-)\left(M\frac{\partial^2 w}{\partial t^2} + C\frac{\partial w}{\partial t}\right) \\ & + \delta(x-L_1)P, \end{aligned} \tag{1}$$

$$\text{for } 0 \leq x \leq L.$$

With the application of the Kronecker Delta function $\delta(x)$, the concentrated mass, mass moment of inertia and dashpot are implemented at the free end of the cantilever beam. The time dependent concentrated load function P is positioned by L_1. By setting L_1 equal to L^- the load is positioned at the tower top.

2.2 Boundary conditions

At $x = 0$, the beam is clamped. The boundary conditions at this position can be formulated as

$$w|_{x=0} = \left.\frac{\partial w}{\partial x}\right|_{x=0} = 0. \tag{2}$$

At the free end, two dynamic boundary conditions are needed to solve the problem. As the rotor properties are already incorporated in equation (1), the conditions can be defined as zero:

$$\left.\frac{\partial^2 w}{\partial x^2}\right|_{x=L} = \left.\frac{\partial^3 w}{\partial x^3}\right|_{x=L} = 0. \tag{3}$$

2.3 Initial conditions

As only the steady state response to load excitation is analyzed, no initial conditions need to be formulated.

3 Analysis procedures

3.1 Modal analysis

The existence of orthogonal modes forms the basis of modal analysis. Due to the presence of the concentrated mass and dashpot at the free end, not all operators in equation (1) are self-adjoint and the derivation of orthogonal modes is a considerable task [8]. Moreover, since the system is damped non-classically, the assumption that the structural motion is dictated by classical normal modes is not valid [2].

Nevertheless, while simply assuming that classical normal modes do exist, exact mode shape expressions can be derived, as was done in [12]. Yang and Wu [15] derived exact eigensolutions by treating the system in a compact spatial state space form. The common practice in software with dynamic applications is even simpler. Mode shapes are estimated by neglecting the disturbing concentrated components. Considering the wind turbine support structure, this comes down to the mode shapes of a cantilever beam.

By defining the mode shape at each natural frequency n as ϕ_n as a function of x, the solution of (1) can be written as

$$w = \sum_{n=1}^{\infty} \phi_n q_n, \tag{4}$$

where q_n is a function of time only. After substitution of (4) into (1), the system of equations can be decoupled into n equations of motion on the basis of modal orthogonality. This is done by multiplication of equation (1) by ϕ_n and subsequent integration of the expression over the length L. The equation of motion per natural mode yields

$$K_n q_n = -M_n \frac{\mathsf{d}^2 q_n}{\mathsf{d}t^2} - C_n \frac{\mathsf{d}q_n}{\mathsf{d}t} + P_n, \tag{5}$$

where K_n, M_n, C_n, and P_n are respectively the generalized stiffness, generalized mass, generalized damping and generalized external force per mode n:

$$K_n = EI \int_0^L \phi_n \frac{\mathsf{d}^4 \phi_n}{\mathsf{d}x^4} \mathsf{d}x, \tag{6}$$

$$M_n = \rho A \int_0^L \phi_n^2 \mathsf{d}x + M\ \phi_n^2\big|_{x=L}, \tag{7}$$

$$C_n = c_d \int_0^L \phi_n^2 \mathsf{d}x + C\ \phi_n^2\big|_{x=L}, \tag{8}$$

$$P_n = P\phi_n\big|_{x=L_1}. \tag{9}$$

As stated before, the general approach to solve equation (5) is by setting the mode shape functions equal to the shape functions of a prismatic cantilever beam, which satisfy the boundary conditions (2) and (3). In order to analyze the resulting system of equations in the frequency domain, integral transformation can be applied.

It should be remembered that the decoupling of (1) took place under the assumption that classical normal modes do exist, despite the presence of nonclassical damping. Though incorrect, this is a common assumption in the evaluation of model analysis and is therefore also employed in this comparative study.

3.2 Direct Fourier transform

Instead of first decoupling equation (1) on the basis of modal orthogonality and subsequently analyze the decomposed system with the help of an integral transformation, the system can also be transformed instantly to an ordinary differential equation. Though transient responses can be analyzed with the help of Laplace transformation, for the current study use is made of Fourier transformation. Doing so, the analyses in this paper are restricted to the steady state response.

In order to evaluate the structural response in the frequency domain, Fourier transformation is applied as follows:

$$\tilde{f}(\omega) = \int_{-\infty}^{\infty} f(t) e^{-i\omega t} \mathsf{d}t, \tag{10}$$

where $f(t)$ represent a function in the time domain and $\tilde{f}(\omega)$ the transformed function in the domain of the excitation frequency ω. i is $\sqrt{-1}$ and ω the excitation frequency.

By applying the integral of equation (10), the partial differential equation (1) can be transformed into the following ordinary differential equation:

$$
\begin{aligned}
EI\frac{\mathrm{d}^4\tilde{w}}{\mathrm{d}x^4} =& \rho A\omega^2\tilde{w} - ic_d\omega\tilde{w} \\
&+ \delta(x-L^-)\left(M\omega^2\tilde{w} - iC\omega\tilde{w}\right) \\
&+ \delta(x-L_1)\tilde{P}, \\
& \\
& \text{for } 0 \leq x \leq L.
\end{aligned}
\tag{11}
$$

4 Reference turbines

The comparative analysis is performed on the basis of three reference turbines: V90-3.0 MW, SWT-3.6-107 and NREL 5-MW. All turbines are oriented horizontally upwind and contain three blades. From [6, 10, 13], the rotor diameter, the operational rotor speed and the total mass of the RNA are obtained. The turbine properties are summed up in Table 1.

The turbines chosen represent three power classes and therefore varying rotor diameters and RNA masses.

4.1 Support structure design

4.1.1 Support structure design frequencies

The design of support structures is based on the operational intervals of the turbine rotor. From these intervals the so-called $1P$ and $3P$ ranges can be derived. $1P$ refers to the passing frequency of each blade separately and $3P$ to the passing frequency of any blade from support structure perspective, given that the turbine is three bladed. Table 2 presents the $1P$ and $3P$ frequency ranges of the three considered turbines.

On the basis of the $1P$ and $3P$ frequency ranges, three support structure design frequency ranges can be distinguished, commonly called the *soft-soft*, *soft-stiff* and *stiff-stiff* frequency range. Design in the *soft-soft* range, meaning a first natural frequency smaller than the $1P$ frequencies, generally results in a highly flexible support structure, and design problems with respect to acceptable deformations are to be expected. Moreover, it is also in this frequency range that sea waves possess the largest amount of energy. Considering this all, it is not very likely that support structures for offshore wind turbines are designed in the *soft-soft* range. The *stiff-stiff* range on the other hand, meaning a first natural frequency larger than the $3P$ frequencies, requires a very stiff foundation. In general, monopile foundations cannot be applied to achieve this requirement. An important premise of this study is that the structural characteristics of the support structure and turbine tower are more or less constant over the length. Monopile designs aiming at too high first natural frequencies require structural dimensions that cannot be produced and installed and are therefore left out of consideration.

The focus of this study is on the *soft-stiff* range. Primarily, all designs are based on the upper bound frequency of the $1P$ range. In order to analyze trends in structural response, the frequency range up to the upper bound of the $3P$ range is considered. Though this range includes frequencies which are undesirable for support structure design, it helps to regard the results in a broader perspective.

4.1.2 Estimation of support structure cross-sectional dimensions

In order to compare the structural response determined with modal analysis to the frequency domain response, structural properties of the support structure need to be established. These properties, which comprise the cross sectional area A and the second moment of area I, can be estimated on the basis of the first natural frequency and the RNA mass. To do so, use is made of the modal analysis procedure, i.e. the natural mode shape of a cantilever beam without top mass.

By setting the D/t ratio at 80 the following relation between the pile diameter and the first natural frequency ω_1 can be derived:

$$
\omega_1^2 = \frac{1}{640}\left[\frac{\pi E D^4 \int_0^L \phi_1 \frac{\mathrm{d}^4\phi_1}{\mathrm{d}x^4}\mathrm{d}x}{\frac{159}{25600}\rho\pi D^2 \int_0^L \phi_1^2 \mathrm{d}x + M\ \phi_1^2|_{x=L}}\right],
\tag{12}
$$

in which D represents the outer diameter of the monopile and tower, t the corresponding wall thickness, and E Young's modulus of both tower and support structure material. [14] presents a value of 80 as initial estimate for the monopile foundation. Though the tower may be produced with a higher D/t ratio, the value of 80 is kept constant over the entire length of the structure.

It should be noted that the dimensions derived represent equivalent values for a prismatic beam structure, as the actual dimensions will vary with height. This simplification affects the modal analysis and frequency domain analysis equally.

Table 1: Properties of the reference turbines.

Turbine type	Rotor diameter [m]	Rotor speed [rpm]	RNA mass [t]
V90-3.0MW	90	8.6-18.4	111
SWT-3.6-107	107	5-13	220
NREL 5-MW	126	6.9-12.1	350

Table 2: $1P$ and $3P$ frequency ranges.

Turbine type	$1P$ range [rad/s]	$3P$ range [rad/s]
V90-3.0MW	0.90-1.93	2.70-5.78
SWT-3.6-107	0.52-1.36	1.57-4.08
NREL 5-MW	0.72-1.27	2.17-3.80

4.1.3 Structural length

Figure 2 shows the composition of the structural length L. This length comprises:

- Tower length, which is build up from the rotor radius and a clearance length.
- Supersea and subsea support structure length, taking into account tidal variations, extreme waves and platform clearance.
- Fixity length, representing the additional length enabling the clamped boundary conditions at $x = 0$.

The lengths chosen typically represent North Sea conditions. In accordance with [5], the fixity length is set at $3.5D$.

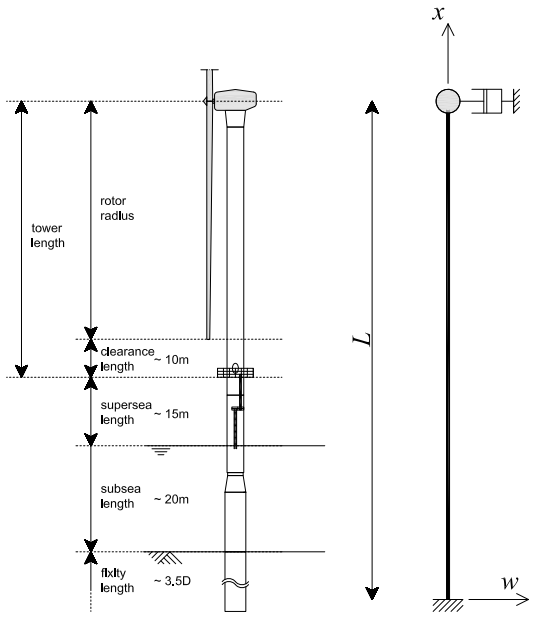

Figure 2: Structural length composition.

4.2 Damping

4.2.1 Aerodynamic damping

Due to the motion of a structural element in fluctuating wind, the actual load the structure experiences is affected. Generally, the load is reduced, or, stated differently, the resistance to motion increases. This phenomenon is called aerodynamic damping. The aero-elastic properties of an operating turbine rotor amplify the significance of this type of damping.

During the preliminary design phase, the turbine rotor is designed separately, under the assumption that the flexible rotor is rigidly fixed at the hub. From this analysis follow the tower top interface forces, which already are corected for aerodynamic damping resulting from rotor blade flexibility. Additional aerodynamic damping follows from rigid body fore-aft motion of the operating rotor. The concentrated dashpot at the tower top (see Figure 1) represents this additional damping.

Proper estimation of the amount of this type of damping still remains a considerable task. Nevertheless, for constant speed turbines a closed form formula is derived [4]. For soft and light support structures, a damping ratio of 4.0% for aerodynamic damping is reasonable to adopt, for stiff structures this value can drop to 1.0% [7, 11]. This damping ratio ξ_1 expresses a percentage with respect to the first mode critical damping $c_{cr;1}$. As for the direct solution in the frequency domain no mode shapes are determined, this damping ratio is translated into an actual damping value, with the help of equation (7) and (8), by

$$C = \frac{\xi_1 c_{cr;1}}{\phi_1^2|_{x=L}} = \frac{2\xi_1 M_1 \omega_1}{\phi_1^2|_{x=L}}. \quad (13)$$

C is determined as 4.0% of $c_{cr;1}$ for the lower bound first natural frequency. If the support structure design is adjusted, the value of C remains unaffected.

4.2.2 Structural damping

Burton et al. [1] suggest a value between 0.5 and 1.0% for structural damping. Again, on this basis an actual damping value can be determined by making use of the generalized damping and generalized mass:

$$c_d = \frac{2\xi_1 M_1 \omega_1}{\int_0^L \phi_1^2 \mathrm{d}x}. \quad (14)$$

For the current evaluations, the first mode damping ratio resulting from structural damping is set at 1.0%.

As for the derived aerodynamic damping it should be noted that equation (13) and (14) make use of inaccurate mode shapes. The damping values derived are affected by this inaccuracy.

4.3 Load positioning

With respect to the location of the oscillating load, two scenarios are distinguished. Firstly, the load is positioned at the tower top $(L_1 = L)$. This scenario represents fluctuating wind load on the rotor. Secondly, the load is positioned at mean sea level. Doing so, the effect of waves or oscillating load effects due to floating ice is simulated. Whereas the first scenario mainly excites the first fore-aft mode of the support structure, from the second mode significant higher mode excitation can be expected.

5 Result comparison

On the basis of the structural characteristics of the turbines, the dynamic amplification of the tower top deflection due to an oscillating load at the tower top is determined. The modal analysis is limited to the response to the first two fore-aft modes. Figure 3 presents the results for varying excitation frequency. The vertical axis gives the actual dynamic amplification, determined by the ratio of the absolute value of the dynamic deflection and the static deflection.

From Figure 3 it follows that the dynamic amplification at the first natural frequency, predicted with the modal analysis, equals the amplification determined with the help of direct Fourier transformation. Also no visual difference between the resonance frequencies themselves can be observed. The latter is obviously not the case for the second resonance frequency, which is shown to be importantly higher when Fourier transformation is applied. This is caused by the poor prediction of the mode shape of the second natural mode in the modal analysis. In estimating the second mode shape, the turbine rotor inertia cannot be neglected. Nevertheless, the structural response at the second natural frequency can be considered as negligibly small. This implies that, considering the first two natural modes, the structural response to tower top loading can be predicted reasonably well by the modal analysis with the estimated mode shapes.

With respect to the three different turbines, no remarkable differences can be identified. In all cases, the first mode dynamic amplification factor is slightly less than 10. Secondly, the second natural frequency is underestimated by the modal analysis approach in each case, whereas the structural response is overestimated in all cases.

When the oscillating load is transferred to mean sea level, resonance peaks are observed at the same natural frequencies. This is shown in Figure 4. Considering peak sizes, there is a remarkable difference. The modal analysis shows to overestimate the dynamic amplification at both the first and the second natural frequency, irrespective of the turbine type. The structural response at the second natural frequency cannot be neglected. As the frequency content of wave loading is mainly concentrated in the lower frequency range, up to 2.5 rad/s, it is unlikely that the second natural mode is to be excited, especially since the actual second natural frequency is even higher than predicted with modal analysis. The fact that wave spectra, like JONSWAP and Pierson Moskowitz, represent linearized wave loading and do not account for breaking waves can, however, not be ignored.

Figure 5 shows the frequency responses due to sea level loading over a frequency bandwidth of 0.50 rad/s in the vicinity of the first natural frequency. These graphs clearly show the difference in dynamic amplification following from both methods. For each turbine, modal analysis overestimates the response compared to the results obtained by

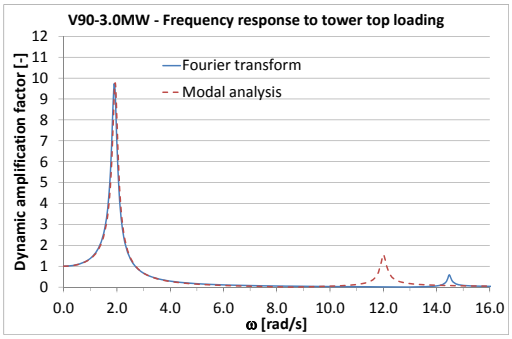

(a)

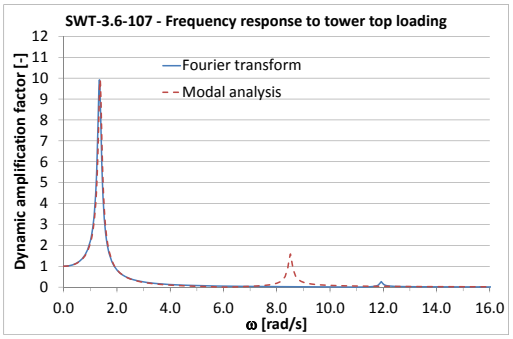

(b)

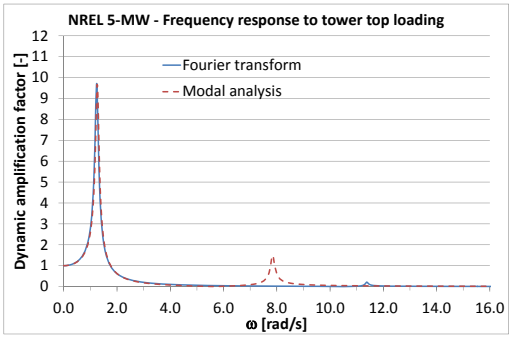

(c)

Figure 3: Dynamic amplification of the tower top deflection due to tower top loading, for the (a) V90-3.0MW, (b) SWT-3.6-107 and (c) NREL 5-MW.

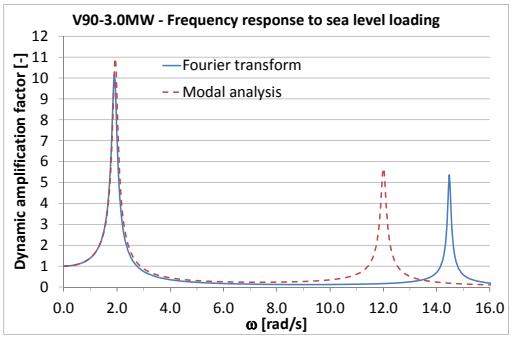

(a)

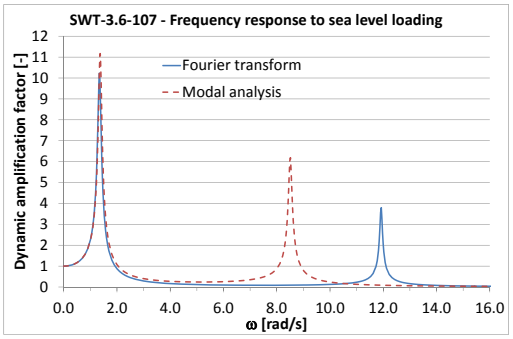

(b)

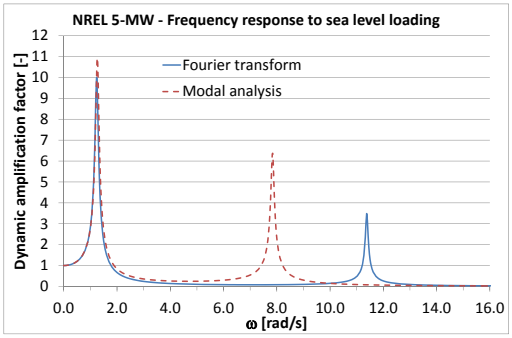

(c)

Figure 4: Dynamic amplification of the tower top deflection due to sea level loading, for the (a) V90-3.0MW, (b) SWT-3.6-107 and (c) NREL 5-MW.

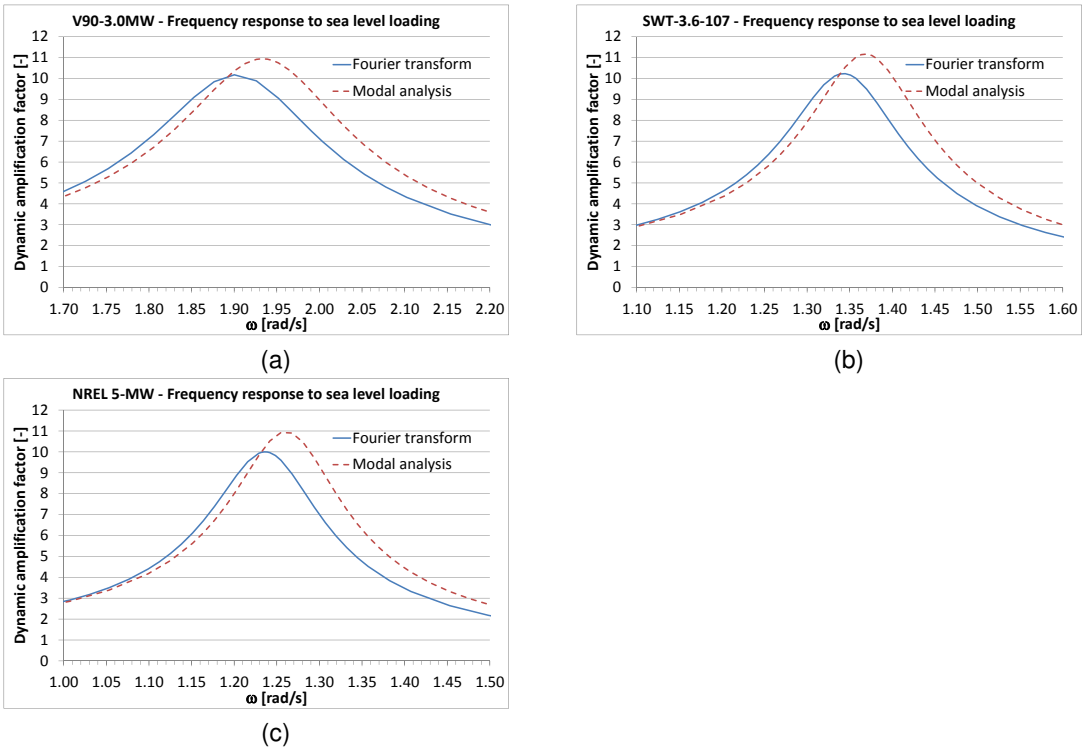

Figure 5: Dynamic amplification at first natural frequency of the tower top deflection due to sea level loading, for the (a) V90-3.0MW, (b) SWT-3.6-107 and (c) NREL 5-MW.

Fourier transformation. The latter approach is most precise. Also a slight overestimation of the first natural frequency becomes visible. These differences instantly follow from the error in the mode shape prediction, by which both the effect of the concentrated load and the effective damping are affected.

Within the limits of the adopt support structure model, the three turbines merely represent different top masses. Besides, due to different rotor velocities, the $1P$ and $3P$ frequency ranges vary, and so do the design values of the first natural frequency. In general, the observed response characteristics for each turbine are equivalent. The most remarkable differences between the results of the analysis procedures are the dynamic amplification due to sea level loading, which is overestimated in all cases by the modal analysis, and the value of the second natural frequency, which is underestimated by the modal analysis in all cases.

By adjusting the support structure design, the first natural frequency can be increased. Figure 6 shows relative differences between the structural response determined with the two analysis procedures for varying first natural frequencies. Firstly, Figure 6(a) presents the development of the maximum dynamic amplification factor determined with modal analysis relative to the factor determined with the help of Fourier transformation. It is shown that for all turbines the ratio between the amplification factors due to tower top excitation is more or less 1.0, irrespective of the first natural frequency of the turbine. When considering sea level excitation, the ratio shows a strong decline for increasing first natural frequencies. This implies that the estimated first natural mode becomes more correct if the stiffness of tower and support structure is enhanced.

Figure 6(b) shows the development of the ratio of the second natural frequencies for increasing first natural frequency. Also here a strong convergence to a ratio 1.0 can be observed, which implies that for a higher first natural frequency, the estimated mode shape becomes more correct. A remarkable aspect of both Figure 6(a) and (b) is that the trendlines for the different turbines are overlapping. All curves follow approximately the same trajectory, which implies that the differences in RNA mass, from 111 t for the V90-turbine to 350 t for the NREL-turbine, do not affect the relative difference between the analy-

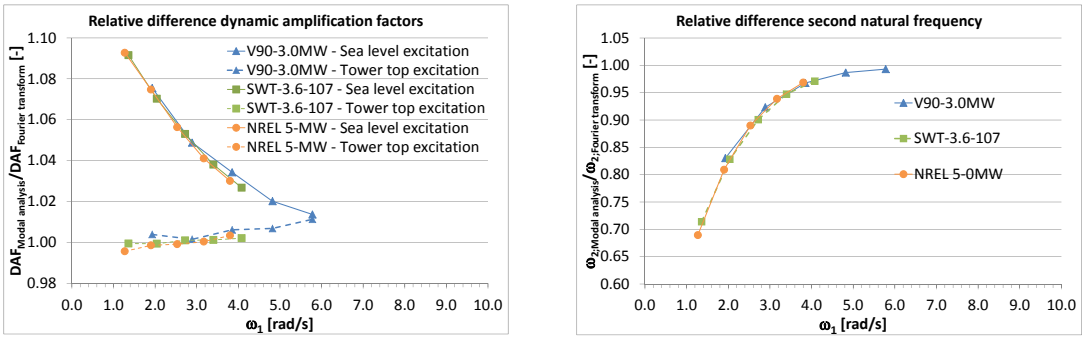

(a) (b)

Figure 6: Relative differences between structural response determined by modal analysis and Fourier transformation as a function of ω_1 of the (a) dynamic amplification factor DAF at the first natural frequency, and (b) second natural frequency ω_2.

sis procedures much.

The first natural frequencies are varied by adjusting the pile diameter D, in accordance with equation (12). In a number of cases, unrealistically large monopile and tower diameters are required to achieve the aimed for natural frequency. Within the limits of this paper this is accepted, as the objective is to explore differences between the two analysis procedures. The overall validity of the fixity length can also be doubted. Nevertheless, this approach is adopted for all support structure designs, as its effect is easily traceable and therefore limitedly disturbing.

6 Conclusions

In preliminary support structure design for offshore wind turbines, fatigue damage can be estimated in the frequency domain. Doing so, commonly modal analysis is applied to determine the structural response. Due to the structural characteristics of a simple wind turbine modal, especially the concentrated RNA mass at the tower top, modal analysis cannot be applied straightforwardly. Use is made of the mode shapes of a cantilever beam, without the concentrated mass.

This paper assesses the effect of these assumed mode shapes, by comparing the structural response of a support structure model for preliminary design determined with modal analysis and with Fourier transformation. The latter analysis procedure can cope with the concentrated RNA mass. The model is kept simple intentionally: prismatic support structure and turbine tower is assumed and the foundation stiffness is taken into account by an additional fixity length. The comparison is done for three turbines, which principally represent different RNA masses. In increasing order: V90-3.0MW, SWT-3.6-107 and NREL 5-MW. With respect to loading scenarios, tower top loading and sea level loading are distinguished.

Considering tower top loading, modal analysis predicts the structural response at the first natural frequency accurately, with a deviation of the dynamic amplification of less than 1%. In case of sea level loading, modal analysis overestimates the first mode structural response for relative soft support structures, up to approximately 9% for the SWT-3.6-107 and NREL 5-MW turbines. Regarding the second natural mode, the natural frequency is generally underestimated, and the dynamic amplification overestimated. The second mode shape estimation can be considered as poor.

It is shown that by increasing the stiffness of tower and support structure, the relative difference between the analysis procedures diminishes. This applies both for the dynamic amplification due to sea level loading and the value of the second natural frequency. Nevertheless, if for economic reasons a relatively soft structure is designed, the more accurate analysis based on Fourier transformation may be worthwhile to consider for fatigue damage estimation. From the overlapping curves in Figure 6 it can be concluded that the difference in RNA mass does not affect the relative difference between the analysis procedures much. This implies that the conclusions drawn on the basis of the observed responses are valid, irrespective of the RNA mass. As the procedures should give the same result for

undamped systems with zero RNA mass, it can be expected that for small tower top masses the observed deviation establishes quickly.

7 Acknowledgements

This work has been supported by the Far and Large Offshore Wind (FLOW) innovation program.

References

[1] T. Burton, N. Jenkins, D. Sharpe, and E. Bossanyi. *Wind energy handbook*. Wiley, West Sussex, UK, second edition, 2011.

[2] T.K. Caughey. Classical normal modes in damped linear dynamic systems. *ASME Journal of Applied Mechanics*, 27:269–271, 1960.

[3] T.K. Caughey and M.E.J. O'Kelly. Classical normal modes in damped linear dynamic systems. *ASME Journal of Applied Mechanics*, 32: 583–588, 1965.

[4] A.D. Garrad. Forces and dynamics of horizontal axis wind turbines. In L.L. Freris, editor, *Wind Energy Conversion Systems*, chapter 5, pages 119–144. Prentice Hall, Englewood Cliffs, New Jersey, 1990.

[5] L.A. Harland and J.H. Vugts. Methods assisting the design of OWECS part C: reliability methods. In Kühn, editor, *Opti-OWECS Final Report*, volume 2. Delft University of Technology, Delft, The Netherlands, 1998.

[6] J. Jonkman, S. Butterfield, W. Musial, and Scott G. Definition of a 5-MW reference wind turbine for offshore system development. Technical Report NREL/TP-500-38060, National Renewable Energy Laboratory, Golden, Colorado, February 2009.

[7] M.J. Kühn. *Dynamics and Design Optimisation of Offshore Wind Energy Conversion Systems*. PhD thesis, Delft University Wind Energy Research Institute, 2001.

[8] L. Meirovitch. *Analytical methods in vibrations*. MacMillan, New York, New York, 1967.

[9] H.H. Pan. Some applications of symbolic functions on beam problems. *Journal of the Franklin Institute*, 275:303–313, 1963.

[10] Siemens AG. New dimensions Siemens Wind Turbine SWT-3.6-107, November 2012. URL `http://www.energy.siemens.com/hq/pool/hq/power-generation/renewables/wind-power/wind%20turbines/E50001-W310-A103-V6-4A00_WS_SWT_3_6_107_US.pdf`.

[11] J. van der Tempel. *Design of Support Structures for Offshore Wind Turbines*. PhD thesis, Delft University Wind Energy Research Institute, 2006.

[12] C.W.S. To. Vibration of a cantilever beam with a base excitation and tip mass. *Journal of Sound and Vibration*, 83(4):445–460, 1982.

[13] Vestas Wind Systems A/S. V90-3.0 MW Exceptional performance and reliability at high-wind-speed sides, November 2012.

[14] W.E. de Vries and V.D. Krolis. Effects of deep water on monopile support structures for offshore wind turbines. In *Proceedings of EWEC 2007*, Milan, Italy, 2007.

[15] B. Yang and X. Wu. Transient response of one-dimensional distributed systems: a closed form eigenfunction expansion realization. *Journal of Sound and Vibration*, 208(5):763–776, 1997.